European Journal of Agronomy 177 (2026) 128106

Contents lists available at ScienceDirect

European Journal of Agronomy

journal homepage: www.elsevier.com/locate/eja

China's spring and summer maize growth exhibit differential sensitivities to recent climate change: Evidence from satellite observations and machine learning

Yang Song [a,1], Wangyipu Li [b,2], Xun Yu [c,3], Xianglin Ji [d,4], Xiaoliang Lu [e,5], Xing Li [f,6], Chao Zhang [a,7], Yong He [a,8], Xiangyuan Wan [a,9,*], Jing Wang [g,10,*]

[a] School of Advanced Agricultural Sciences, University of Science and Technology Beijing, Beijing 100096, China
[b] Institute of Remote Sensing and Geographic Information System, School of Earth and Space Sciences, Peking University, Beijing 100871, China
[c] Institute of Crop Sciences, Chinese Academy of Agricultural Sciences, Beijing 100081, China
[d] State Key Laboratory of Earth Surface Processes and Disaster Risk Reduction, Faculty of Geographical Science, Beijing Normal University, Beijing 100875, China
[e] State Key Laboratory of Soil Erosion and Dryland Farming on the Loess Plateau, Northwest A&F University, Yangling 712100, China
[f] School of Geography and Planning, Sun Yat-sen University, Guangzhou 510275, China
[g] College of Resources and Environmental Sciences, China Agricultural University, Beijing 100193, China

ARTICLE INFO

Keywords:
Climate change
Smart agriculture
Environmental stress
Remote sensing
Random forest

ABSTRACT

Over the past few decades, China has been engaged in improving maize (*Zea mays* L.) production to ensure food security. However, it remains unclear whether the spring and summer maize planting regions had different responses to a changing climate. Therefore, this study aims to use smart agricultural techniques to analyze the sensitivities of maize growth to recent climate change in China during 2000–2020. The main objectives are to reveal differences in the relationship between climate and agriculture across the two regions, and to provide insights into optimizing agronomic practices in space and time. Satellite-based observations indicated that summer maize faced more challenging growth conditions (i.e., significant warming and drying) than spring maize during the last two decades. However, as the spring maize regions shifted toward favourable cooler and wetter conditions, its growth and yield increase rates were mostly higher than those of summer maize. To estimate the sensitivities of maize growth to climate factors and atmospheric carbon dioxide concentration (CO_2), we employed random forest-based simulation experiments. The results demonstrated that spring maize growth was more sensitive to climate and CO_2 than summer maize during the period. We found that the sensitivities were significantly different between the two regions. It seems that spring maize growth was more sensitive, likely due to its predominantly rain-fed nature, making it more vulnerable to climate fluctuations. Conversely, summer maize showed greater resistance, likely buffered by more well-developed irrigation facilities, allowing it to withstand adverse environments. Specifically, spring maize's high sensitivity to water supply illustrates the necessity of expanding irrigation to mitigate extreme events, while summer maize's exposure to heat stress calls for the deployment of heat-tolerant hybrids. These findings provide an evidence-based framework for region-

* Corresponding authors.
E-mail addresses: songyang@ustb.edu.cn (Y. Song), lwyp_sess@stu.pku.edu.cn (W. Li), 82101211308@caas.cn (X. Yu), xianglin_ji@mail.bnu.edu.cn (X. Ji), luxiaoliang@nwafu.edu.cn (X. Lu), lixing58@mail.sysu.edu.cn (X. Li), zhangchao7@ustb.edu.cn (C. Zhang), heyong01@ustb.edu.cn (Y. He), wanxiangyuan@ustb.edu.cn (X. Wan), wangj@cau.edu.cn (J. Wang).
[1] 0000–0002-4233–2682
[2] 0000–0003-1960–3517
[3] 0000–0002-1780–7711
[4] 0000–0002-8646–146X
[5] 0000–0002-9416–9813
[6] 0000–0003-2206–0429
[7] 0000–0002-1172–056X
[8] 0000–0003-4062–9201
[9] 0000–0002-5939–4847
[10] 0000–0002-7960–0396

https://doi.org/10.1016/j.eja.2026.128106
Received 4 November 2025; Received in revised form 4 March 2026; Accepted 24 March 2026
Available online 27 March 2026

specific adaptation strategies, such as breeding improved plant architecture, optimizing planting density, and promoting the northward expansion of cropping systems, thereby ensuring crop yield stability under diverse climate challenges. Overall, this study provides decision-makers with essential support for developing adaptation strategies, highlighting the differential impacts of climate change on crops across various regions.

1. Introduction

Maize (*Zea mays* L.) is essential to global food security and economic growth. China ranks as the world's 2nd largest producer with planting widespread across the country. Although some reports suggest that climate change may not always have negative impacts on crop growth, it is clear that elevated temperatures, extreme weather events, and others continue to introduce uncertainty into maize yield increases (Huang et al., 2021; Rezaei et al., 2023; Tao et al., 2015). Previous studies found that crop growth exhibits spatially heterogeneous responses to a changing climate (Lobell and Azzari, 2017; Lu et al., 2025; Zhao and Lobell, 2017). Especially for spring and summer maize, the climatic conditions they experienced could be markedly different (Wang et al., 2022). Given the northward expansion of China's summer maize cropping system, optimizing planting zones will become crucial for ensuring sustained yield growth (Yang et al., 2015). However, spring and summer maize growth' sensitivities to recent climate change remain unclear, making it difficult to distinguish differences between them. The results derived from meteorological stations and crop models suggest that they may exhibit different sensitivities to environmental factors (Huang et al., 2021; Tao et al., 2015), but it remains challenging in characterizing their spatiotemporal patterns across a wide geographic range.

Satellite observations and their derived products provide valuable opportunities for monitoring crop growth at large scales. For example, Normalized Difference Vegetation Index (NDVI) can capture crop growth dynamics (Song et al., 2024a; Wan et al., 2022). Solar-Induced chlorophyll Fluorescence (SIF) is considered to be more effective than other indicators in evaluating vegetation growth responses to heat stress, drought, and other extreme events (Geng et al., 2025; Song et al., 2018). Gross Primary Productivity (GPP) is considered to be directly related to crop yield. The synergistic use of satellite-derived GPP and harvest index is able to estimate crop yields across a large region (Yu et al., 2024). Compared to field trials, these satellite-based datasets offer broad spatial coverage, long-term temporal continuity, and consistent measurement standards. In addition, a few studies used satellite observations, meteorological data, and statistical information to develop gridded crop yield products (Cao et al., 2025; Iizumi and Sakai, 2020). These crop yield datasets provide more details on spatial distribution than statistical yearbooks. In recent years, with the popular use of artificial intelligence (AI) algorithms such as machine learning, these vast amounts of data can be well-integrated for modeling purposes, providing a robust framework for understanding crop-environment interactions under recent climate change (Alimagham et al., 2025; Cai et al., 2019).

The sensitivities of vegetation growth to environmental factors were highly heterogeneous across different research (Song et al., 2022; Yuan et al., 2019). Rather than attempting to accurately estimate those constantly changing sensitivities, it is more important to explore the knowledge hidden behind these uncertainties. In this study, we aim to quantify potential differences between the sensitivities of spring and summer maize growth to recent climate change using satellite-based observations and machine learning algorithms. We tracked the trends in mean air temperature (TMP), precipitation accumulation (PRE), vapor pressure deficit (VPD), downward surface shortwave radiation (SRAD), soil moisture (SM), and atmospheric carbon dioxide concentration (CO_2) to evaluate the differences between spring and summer maize planting regions during 2000–2020. Moreover, we illustrated spatiotemporal patterns of NDVI, SIF, and GPP to investigate whether there were differential trends in spring and summer maize growth during this period. We also incorporated the gridded maize yield data to support the satellite observation-derived results. Furthermore, we employed random forest (RF) models to simulate crop growth proxies and yield. By constructing the baseline and factorial simulations, we estimated the sensitivities of NDVI, SIF, GPP, and yield to TMP, PRE, VPD, SRAD, SM, and CO_2 for China's spring and summer maize planting areas during 2000–2020. We conducted statistical difference tests on these estimates to determine whether China's spring and summer maize growth exhibited differential sensitivities to recent climate change. Our findings, derived from satellite observations and machine learning, are expected to provide strong evidence for evaluating differential climate change impacts on agricultural production, underscoring the need for decision-makers to develop adaptation strategies adapted to local conditions.

2. Materials and methods

Spring maize is mostly cultivated in regions practicing a single-season cropping system, while summer maize is usually harvested in areas adopting a double-season cropping system. The active growing seasons for spring and summer maize were defined as May to September and June to September, respectively (Niu et al., 2022). The gridded maize harvest area data were derived from the Spatial Production Allocation Model (SPAM) 2000, 2005, 2010, and 2020 datasets (https://www.mapspam.info). To reduce the uncertainty due to changes in crop types, we used the intersection of maize harvest areas derived from these four SPAM datasets (Fig. 1a). The annual maize harvest area and yield data for each provincial- and prefectural-level region were collected from statistical yearbooks. The preliminary results indicated that our study region produced approximately 88% of China's maize in 2020, enabling it to be representative (Fig. 1b).

The monthly gridded TMP, PRE, VPD, SRAD, and SM data were acquired from TerraClimate (Abatzoglou et al., 2018). We obtained the atmospheric CO_2 mole fraction data from CarbonTracker (CT2022) (Jacobson et al., 2023). The monthly gridded NDVI, SIF, and GPP were used as proxies for maize growth. The NDVI data were derived from MOD13C2 (https://doi.org/10.5067/MODIS/MOD13C2.006). We acquired the SIF data from a high-resolution product, GOSIF (Li and Xiao, 2019). The GPP data were acquired from Bi et al. (2022). In addition, we used the global dataset of historical yields for major crops (GDHY) (Iizumi and Sakai, 2020) and the global yields of four major crops at 5-minute resolution dataset (GlobalCropYield5min) (Cao et al., 2025) for the periods 2000–2016 and 2000–2015, respectively. All datasets described above were first aggregated to monthly means. Subsequently, they were resampled to a spatial resolution of 0.05° using the nearest-neighbor resampling method. We calculated both the mean and maximum growing-season values for NDVI, SIF, and GPP to test the robustness of using a fixed-length growing season for trend analysis.

The Theil-Sen estimator with the non-parametric Mann-Kendall test was used to estimate the linear trends. We deployed this method to evaluate changes in climate factors, CO_2, and maize growth indicators (i.e., NDVI, SIF, and GPP) pixel by pixel during 2000–2020. Using the linear least squares regression method with a two-tailed *t*-test, we estimated the prefecture-level maize yield trends. The Mann-Whitney *U* test was used to identify significant differences between spring and summer maize planting areas, since most of our data did not follow a normal distribution.

To estimate the sensitivities of maize growth to climate and CO_2, we designed two machine learning-based simulation experiments by

building RF models (Liu et al., 2019; Yuan et al., 2019). To further prevent overfitting caused by high dimensionality, monthly data were aggregated into growing-season mean values rather than being treated as independent features. The models were constructed independently for each grid cell and trained using a 70%/30% train/test set split ratio combined with 5-fold cross-validation to ensure robust evaluation under limited temporal samples. Each RF model consisted of 200 trees, with one-third of predictors randomly selected at each split and a minimum leaf size of 5. Trees were grown to full depth, as the risk of overfitting is inherently mitigated by the algorithm's bootstrap aggregation and feature randomness. These hyperparameters were selected based on convergence diagnostics of the out-of-bag error and computational efficiency considerations.

RF_{ALL} served as the baseline simulation where all variables varied with time to predict NDVI, SIF, GPP, or yield. The factorial simulations were conducted by reusing the pre-trained RF_{ALL} model. Specifically, we fixed one target driver (i.e., TMP, PRE, VPD, SRAD, SM, or CO_2) at its year-2000 level while allowing others to vary, generating new predictions without retraining. For example, RF_{TMP} run kept TMP constant at the values in 2000 and varied the other drivers. This machine learning-based simulation framework helps reduce uncertainties arising both from variations in the number of independent variables and from unaccounted management factors (e.g., crop varieties, planting density, irrigation, and fertilization) constrained by data availability. On this basis, we estimated the sensitivities of maize growth to TMP, PRE, VPD, SRAD, SM, and CO_2 as described by the following equations:

$$\Delta Y_{(RF_{ALL}-RF_{TMP})} = \beta_{TMP} \times \Delta TMP_{(RF_{ALL}-RF_{TMP})} + \varepsilon \quad (1)$$

$$\Delta Y_{(RF_{ALL}-RF_{PRE})} = \beta_{PRE} \times \Delta PRE_{(RF_{ALL}-RF_{PRE})} + \varepsilon \quad (2)$$

$$\Delta Y_{(RF_{ALL}-RF_{VPD})} = \beta_{VPD} \times \Delta VPD_{(RF_{ALL}-RF_{VPD})} + \varepsilon \quad (3)$$

$$\Delta Y_{(RF_{ALL}-RF_{SRAD})} = \beta_{SRAD} \times \Delta SRAD_{(RF_{ALL}-RF_{SRAD})} + \varepsilon \quad (4)$$

$$\Delta Y_{(RF_{ALL}-RF_{SM})} = \beta_{SM} \times \Delta SM_{(RF_{ALL}-RF_{SM})} + \varepsilon \quad (5)$$

$$\Delta Y_{(RF_{ALL}-RF_{CO2})} = \beta_{CO2} \times \Delta CO2_{(RF_{ALL}-RF_{CO2})} + \varepsilon \quad (6)$$

where $\Delta Y_{(RF_{ALL}-RF_{TMP})}$, $\Delta Y_{(RF_{ALL}-RF_{PRE})}$, $\Delta Y_{(RF_{ALL}-RF_{VPD})}$, $\Delta Y_{(RF_{ALL}-RF_{SRAD})}$, $\Delta Y_{(RF_{ALL}-RF_{SM})}$, and $\Delta Y_{(RF_{ALL}-RF_{CO2})}$ represent the differences of NDVI, SIF, GPP, and yield between two simulation experiments, respectively, RF_{ALL} is the normal model run, RF_{TMP}, RF_{PRE}, RF_{VPD}, RF_{SRAD}, RF_{SM}, and RF_{CO2} are the model runs that hold one driver constant at its year-2000 level while changing the other variables, respectively, the regression coefficients, β_{TMP}, β_{PRE}, β_{VPD}, β_{SRAD}, β_{SM}, and β_{CO2}, represent the sensitivities to TMP, PRE, VPD, SRAD, SM, and CO_2, respectively, $\Delta TMP_{(RF_{ALL}-RF_{TMP})}$, $\Delta PRE_{(RF_{ALL}-RF_{PRE})}$, $\Delta VPD_{(RF_{ALL}-RF_{VPD})}$, $\Delta SRAD_{(RF_{ALL}-RF_{SRAD})}$, $\Delta SM_{(RF_{ALL}-RF_{SM})}$, and $\Delta CO2_{(RF_{ALL}-RF_{CO2})}$ represent the differences of TMP, PRE, VPD, SRAD, SM, and CO_2 between two simulation experiments, respectively, and ε is the residual error term.

3. Results

3.1. Recent climate and CO_2 trends across China's maize planting areas

This study estimated the trends in climate and CO_2 across China's spring and summer maize planting areas during 2000–2020. We found that the recent trends in climate and CO_2 between the spring and summer maize planting regions were significantly different during the period. Specifically, 52.52% and 95.22% of spring and summer maize planting grid cells, respectively, exhibited an increase in TMP (Fig. 2a). Only 0.56% of spring maize planting areas experienced a significant increase ($p < 0.05$), whereas the proportion of summer maize planting areas reached 13.87%. The significant trends in TMP for spring and summer maize planting regions were –0.01 ± 0.03 and 0.05 ± 0.01 ℃ yr^{-1}, respectively. These significant trends in TMP between the two regions showed a significant difference in statistical distribution ($p < 0.001$) (Fig. S1a). Moreover, we found that more grid cells in spring maize planting areas exhibited increases in PRE and SM (89.54% and 76.94%) (36.26% and 17.83% were significant, respectively, $p < 0.05$) compared to those in summer maize planting areas (39.87% and 38.46%) (1.42% and 10.89% were significant, respectively, $p < 0.05$) (Fig. 2b & e). The significant trends in PRE and SM between the two regions also showed a significant different distribution ($p < 0.001$) (Fig. S1b & e). The significant trends in PRE for spring and summer maize planting regions were 1.65 ± 0.32 and –1.64 ± 1.52 mm yr^{-1}, respectively. The significant trends in SM for spring and summer maize planting regions were 0.29 ± 0.51 and 1.10 ± –0.79 mm yr^{-1}, respectively. For the two regions, 44.76% and 0.01% displayed a significant decline in VPD ($p < 0.05$), while 37.54% and 0.67% had a significant decrease in SRAD, respectively (Fig. 2c & d). The significant trends in VPD for spring and summer maize planting regions were –0.00 ± 0.01 and 0.00 ± 0.00 kPa yr^{-1}, respectively. The significant trends in SRAD between the two regions showed a statistically significant different distribution ($p < 0.001$) (Fig. S1d). The significant trends in SRAD for spring and summer maize planting regions were –0.72 ± 0.34 and 0.32 ± 0.59 W m^{-2} yr^{-1}, respectively. However, there were only a few grid cells within the summer maize growing region where VPD trends passed the significance test, and thus no significant difference was found ($p > 0.05$) (Fig. S1c). In addition, we analyzed CO_2 trends across China's

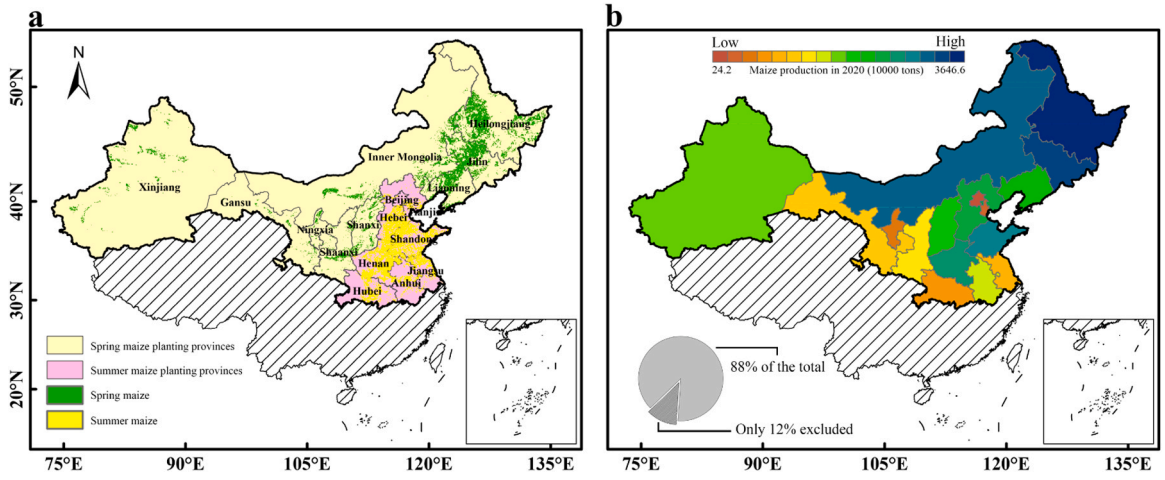

Fig. 1. Spatial distribution of maize planting areas in China. (a) Spring and summer maize planting areas within the study region. (b) Total maize production in 2020 across provinces within the study area.

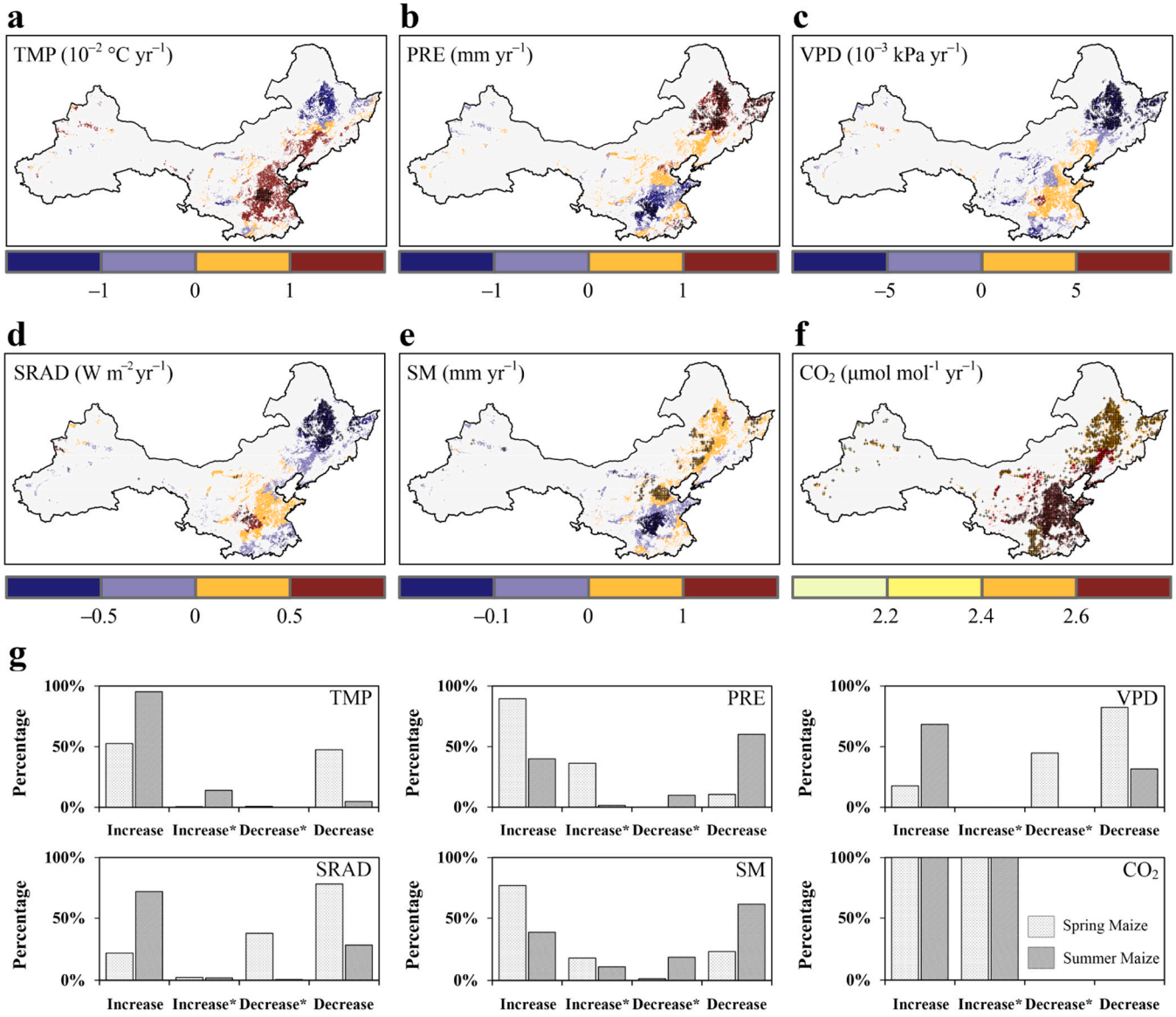

Fig. 2. Spatiotemporal patterns of climate and CO_2 for spring and summer maize planting areas in China during 2000–2020. (a–f) Spatial distribution of the trends in TMP, PRE, VPD, SRAD, SM, and CO_2. The black cross in (a–f) denotes a statistically significant trend ($p < 0.05$). (g) Relative frequency distribution of significant ($p < 0.05$) and non-significant ($p > 0.05$) trends.

maize planting areas during 2000–2020. As expected, atmospheric CO_2 concentrations was significantly elevated in both regions (Fig. 1f), but the increase rate was higher in summer maize planting areas (2.73 ± 0.14 μmol mol^{-1} yr^{-1}) than in the spring maize planting areas (2.38 ± 0.15 μmol mol^{-1} yr^{-1}) (Fig. S1f).

3.2. Spatiotemporal patterns of maize growth under recent climate change

To illustrate the spatiotemporal patterns of spring and summer maize growth, we used satellite observations as key proxies, including NDVI, SIF, and GPP. The results showed that NDVI, SIF, and GPP were increasing in most maize planting areas in China during 2000–2020. Specifically, 84.76%, 91.27%, and 92.75% showed an increase in growing-season mean NDVI, SIF, and GPP (53.57%, 69.55%, and 67.44% were significant, $p < 0.05$), while only 3.06%, 1.68%, and 1.28% recorded a significant decrease, respectively (Fig. 3a–c & g). For the spring maize planting region, 95.53%, 97.42%, and 97.87% experienced an upward trend in NDVI, SIF, and GPP (75.62%, 87.69%, and 91.73% were significant, $p < 0.05$), respectively. For the summer maize planting region, we observed that 72.57%, 84.17%, and 86.87% experienced an upward trend in NDVI, SIF, and GPP (28.13%, 48.62%, and 39.53% were significant, $p < 0.05$), respectively. The significant trends between the two regions showed a significant difference in statistical distribution ($p < 0.001$) (Fig. S2a–c). The rates of increase in NDVI, SIF, and GPP for spring planting areas were generally greater compared to summer planting areas. In addition, we used the growing-season maximum NDVI, SIF, and GPP values to further test the above results (Fig. 3d-f & g). The significant trends between the two regions also showed a significant difference in statistical distribution ($p < 0.001$) (Fig. S2d-f).

We also used the crop yield data from gridded products and statistical yearbooks to further strengthen our findings. Similarly, we evaluated the trends in maize yield per unit area at each grid cell within the period. The results indicated that maize yields were increasing across most parts of China. Specifically, the GDHY-based results showed that 95.47% and 92.52% exhibited an increase in spring and summer maize yields during 2000–2016 (80.74% and 62.24% were significant, $p < 0.05$), respectively (Fig. 4a). The GlobalCropYield5min-based

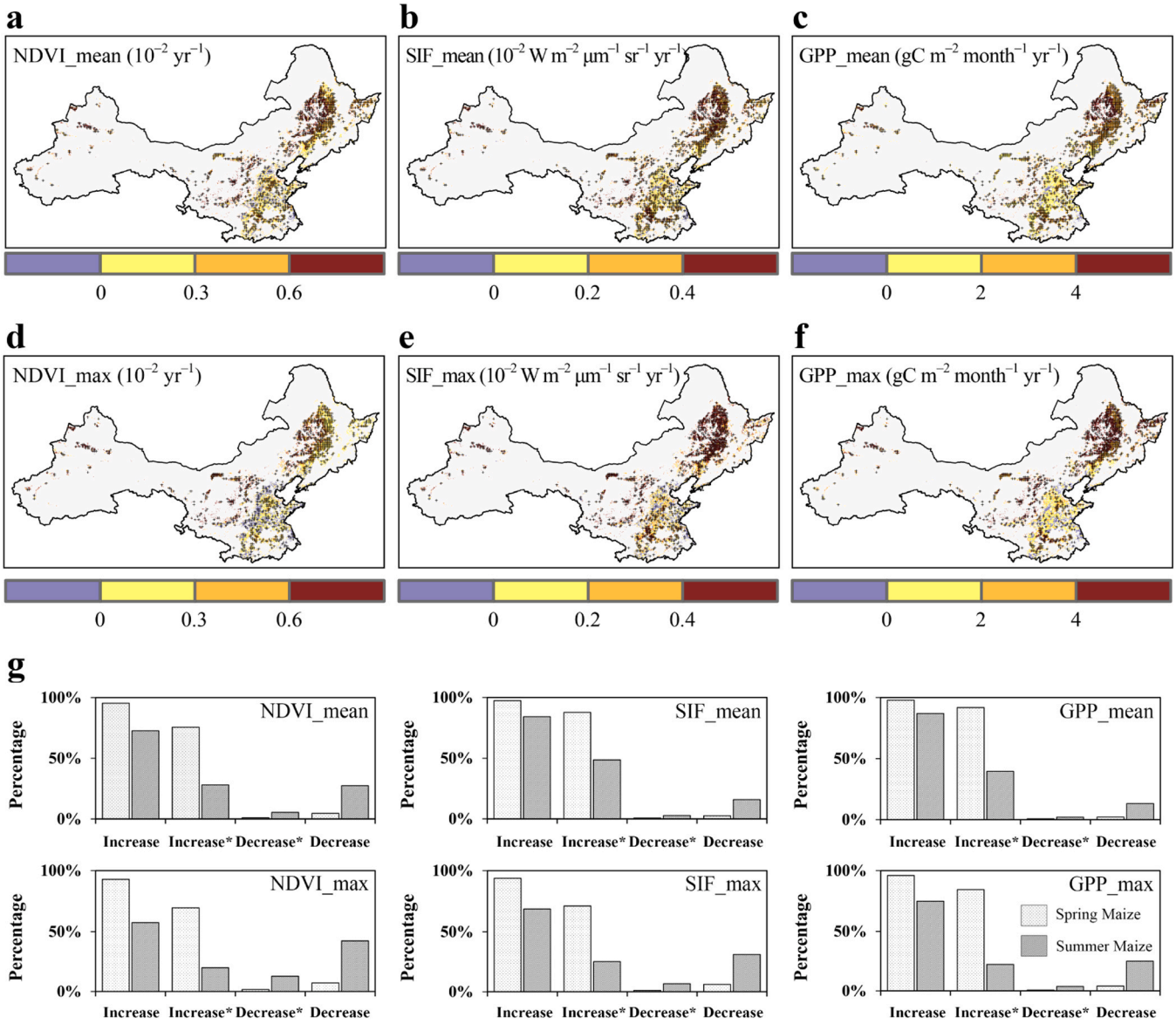

Fig. 3. Spatiotemporal patterns of NDVI, SIF, and GPP for spring and summer maize planting areas in China during 2000–2020. (a–c) Spatial distribution of the trends in maize growing-season mean NDVI, SIF, and GPP. (d–f) Spatial distribution of the trends in maize growing-season maximum NDVI, SIF, and GPP. The black cross in (a–f) denotes a statistically significant trend ($p < 0.05$). (g) Relative frequency distribution of significant ($p < 0.05$) and non-significant ($p > 0.05$) trends.

results showed that 85.27% and 90.70% experienced an increase in spring and summer maize yields during 2000–2015 (46.11% and 33.61% were significant, $p < 0.05$), respectively (Fig. 4b). These two gridded datasets demonstrated increases in spring and summer maize yields, with few statistically significant declines observed. However, they disagreed on the percentage of significant increases, suggesting the uncertainty surrounding current gridded crop yield products (Fig. 4d). In addition, we found that maize yield was increasing in more than 65% of prefecture-level administrative regions (approximately 25% were significant, $p < 0.05$) (Fig. 4c). The percentages of trends in spring and summer maize yields derived from statistical yearbooks were unexpectedly consistent. The significant trends in maize yield between the two regions derived from the GDHY and GlobalCropYield5min datasets showed a statistically significant different distribution ($p < 0.001$), whereas statistical yearbook-based results did not ($p > 0.05$) (Fig. S3).

3.3. Sensitivities of maize growth to climate and CO_2 derived from machine learning

To further analyze maize growth responses to recent climate change, we applied random forest-based models to estimate the sensitivities of growing-season mean NDVI, SIF, and GPP to climate and CO_2 for each grid cell in China during 2000–2020. The random forest models can effectively explain the interannual changes in maize growth for each grid cell (Fig. S4). Our results showed that spring and summer maize growth exhibited differential sensitivities to TMP, PRE, VPD, SRAD, SM, and CO_2. Generally, the mean sensitivities of NDVI, SIF, and GPP to TMP, VPD, and SRAD were negative, while those to PRE, SM, and CO_2 were positive (Table 1). During the period, China's spring maize growth was mostly more sensitive to these drivers than summer maize.

Fig. 5 illustrates the spatiotemporal patterns of NDVI, SIF, and GPP to TMP, PRE, VPD, SRAD, SM, and CO_2 for spring and summer maize planting areas in China during 2000–2020. Specifically, the three maize growth proxies (i.e., NDVI, SIF, and GPP) showed inconsistent spatial

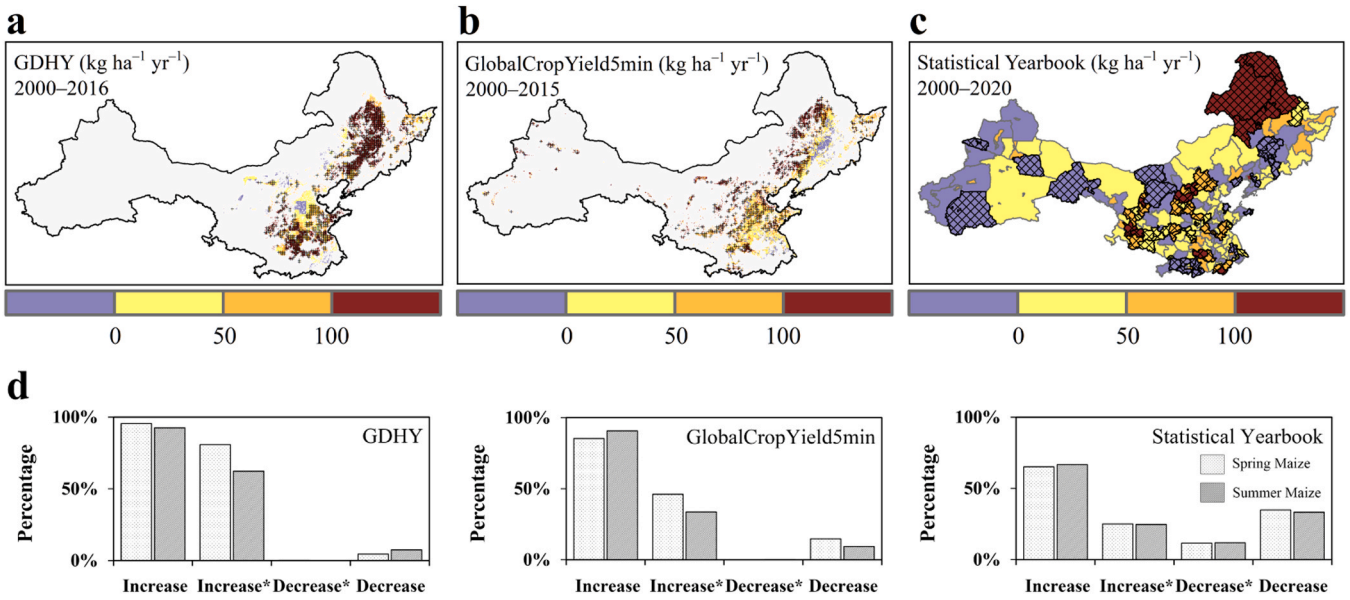

Fig. 4. Spatiotemporal patterns of spring and summer maize yield in China. (a) Spatial distribution of the trends in maize yield derived from GDHY during 2000–2016. (b) Spatial distribution of the trends in maize yield derived from GlobalCropYield5min during 2000–2015. The black cross in (a & b) denotes a statistically significant trend ($p < 0.05$). (c) Spatial distribution of the trends in maize yields collected from statistical yearbooks during 2000–2020. The black grid in (c) denotes a statistically significant trend ($p < 0.05$). (g) Relative frequency distribution of significant ($p < 0.05$) and non-significant ($p > 0.05$) trends.

Table 1
Sensitivities of maize growth to climate and atmospheric CO_2 in the spring and summer planting regions of China, 2000–2020.

ProxyType Variable	NDVI		SIF (W m^{-2} μm^{-1} sr^{-1})		GPP (gC m^{-2} month^{-1})	
	Spring	Summer	Spring	Summer	Spring	Summer
TMP (°C)	−0.0029 ± 0.0053	−0.0011 ± 0.0051	−0.0001 ± 0.0027	−0.0018 ± 0.0044	−0.0008 ± 0.002	−0.0020 ± 0.0030
PRE (mm)	0.0002 ± 0.0003	0.0001 ± 0.0002	0.0001 ± 0.0002	0.0001 ± 0.0001	0.0001 ± 0.0001	0.0001 ± 0.0001
VPD (kPa)	−0.0624 ± 0.0459	−0.0066 ± 0.0281	−0.0329 ± 0.0287	−0.0084 ± 0.0189	−0.0338 ± 0.0243	−0.0077 ± 0.0140
SRAD (W m^{-2})	−0.0004 ± 0.0005	−0.0002 ± 0.0003	− 0.0002 ± 0.0003	−0.0001 ± 0.0002	− 0.0002 ± 0.0003	−0.0001 ± 0.0002
SM (mm)	0.0004 ± 0.0021	0.0001 ± 0.0003	0.0002 ± 0.0014	0.0001 ± 0.0002	0.0002 ± 0.0009	0.0001 ± 0.0002
CO_2 (μmol mol^{-1})	0.0007 ± 0.0005	0.0002 ± 0.00003	0.0005 ± 0.0003	0.0002 ± 0.0003	0.0004 ± 0.0002	0.0002 ± 0.0002

patterns of their sensitivities to TMP. We found widespread negative NDVI sensitivities to TMP (Fig. 5a), while SIF and GPP sensitivities to TMP showed no discernible pattern (Fig. 5 g & m). The sensitivities of NDVI, SIF, and GPP to PRE, SM, and CO_2 were almost positive across China's maize planting areas. In contrast, the sensitivities of NDVI, SIF, and GPP to VPD were nearly all negative. Similarly, except for a few areas, most NDVI, SIF, and GPP showed negative sensitivities to SRAD. Overall, NDVI, SIF, and GPP exhibited negative sensitivities to three of the six drivers (i.e., TMP, VPD, and SRAD) and positive sensitivities to the other three (i.e., PRE, SM, and CO_2). This was in line with our understanding and the mean sensitivities of the two regions in Table 1. Moreover, we deployed the Mann-Whitney *U* test to analyze whether there were differences in the sensitivities between the spring and summer maize planting regions (Fig. S5). The results indicated that the sensitivities between the two regions were all significantly different in their statistical distributions ($p < 0.001$).

Furthermore, we quantified the sensitivities of China's maize yield to TMP, PRE, VPD, SRAD, SM, and CO_2 for each grid cell within the study period (Fig. 6). The sensitivities to TMP and SRAD were negative in the southern spring and northern summer planting regions but positive in most other areas. In contrast, the sensitivities to PRE and SM were positive in these zones. The sensitivities to VPD differed markedly between the spring and summer maize planting regions, being mostly negative for spring maize but nearly all positive for summer maize. Both spring and summer maize yields showed consistently positive sensitivities to CO_2. These results based on gridded yield data were comparable to those derived from satellite observations. However, due to the shorter available time series for these yield data, the spatiotemporal patterns of maize growth's sensitivities to climate and CO_2 derived from these two types of data were not entirely consistent. Nevertheless, China's spring and summer maize yields still exhibited significantly different sensitivities to TMP, PRE, VPD, SRAD, SM, and CO_2 in their statistical distributions ($p < 0.001$) (Fig. S6).

4. Discussion

Our results confirmed that there were large differences in the climate and CO_2 trends between the spring and summer maize planting regions in China during 2000–2020. We found that China's spring maize experienced less warming during its growing season, even showing a decrease in mean growing-season TMP in more northern planting areas. Meanwhile, water availability for spring maize growth in most of these areas could be improved due to increased PRE and SM. It appears that China's spring maize planting areas have experienced a shift toward cooler and wetter conditions (Wen et al., 2019; Zhou et al., 2020b). Against this, we observed impressive increases in TMP across the entire summer maize planting region. Even neighboring southern spring maize growing areas were emerging warming trends, suggesting a potential northward expansion of multiple cropping systems incorporating summer maize (Gao et al., 2019). Lower PRE with related declines in SM made the region more dependent on irrigation, thereby heightening drought risks (Liu et al., 2025c). The non-significant increase in VPD may be attributed to the concurrent rise in saturated and actual vapor pressure (Dong et al., 2024). The surface dimming and subsequent shift

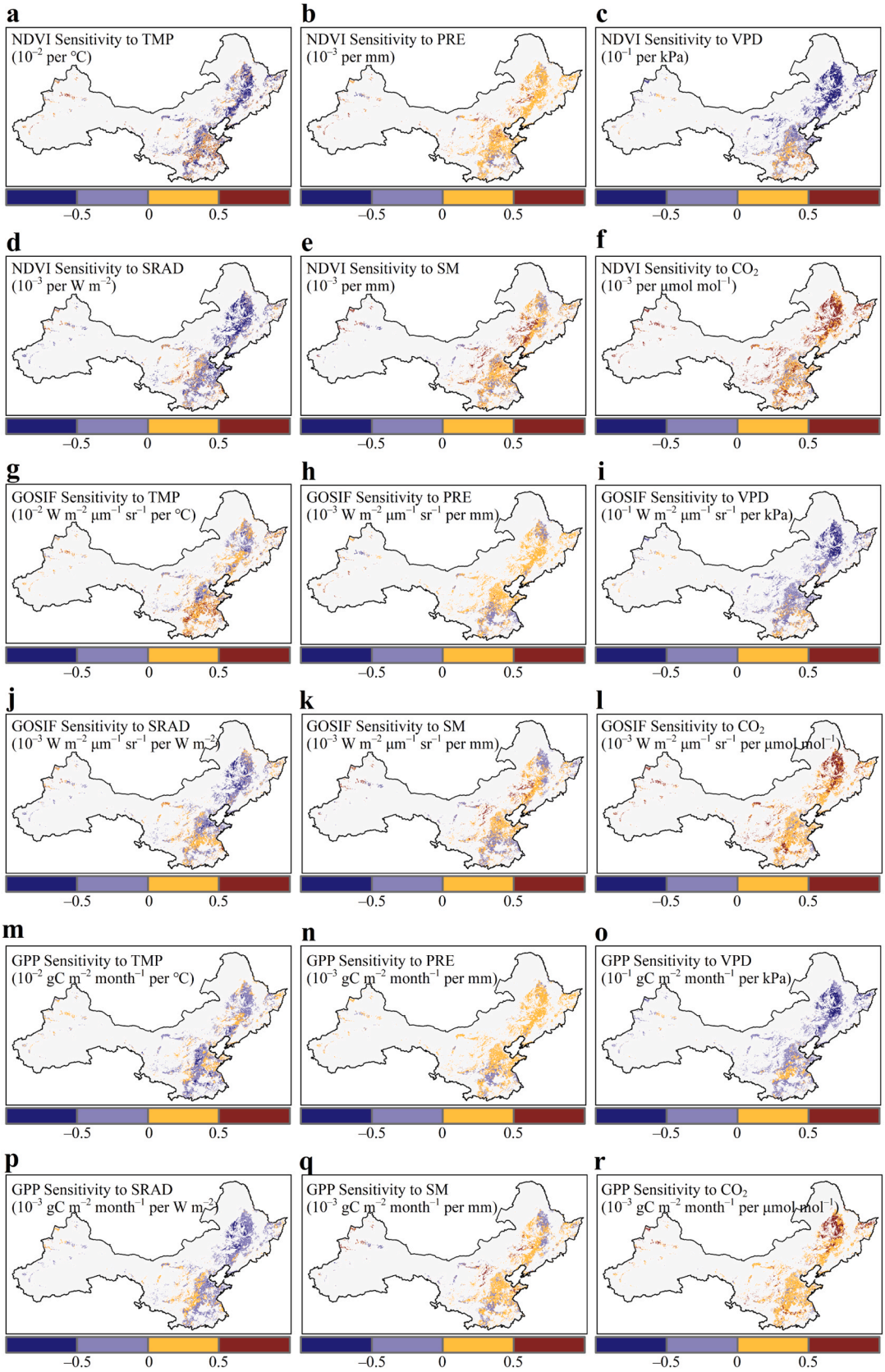

Fig. 5. Spatiotemporal patterns of NDVI, SIF, and GPP sensitivities to TMP, PRE, VPD, SRAD, SM, and CO_2 for spring and summer maize planting areas in China during 2000–2020. (a–f) Spatial distribution of the spring and summer maize's NDVI sensitivities to TMP, PRE, VPD, SRAD, SM, and CO_2. (g–l) Spatial distribution of the spring and summer maize's SIF sensitivities to TMP, PRE, VPD, SRAD, SM, and CO_2. (m–r) Spatial distribution of the spring and summer maize's GPP sensitivities to TMP, PRE, VPD, SRAD, SM, and CO_2.

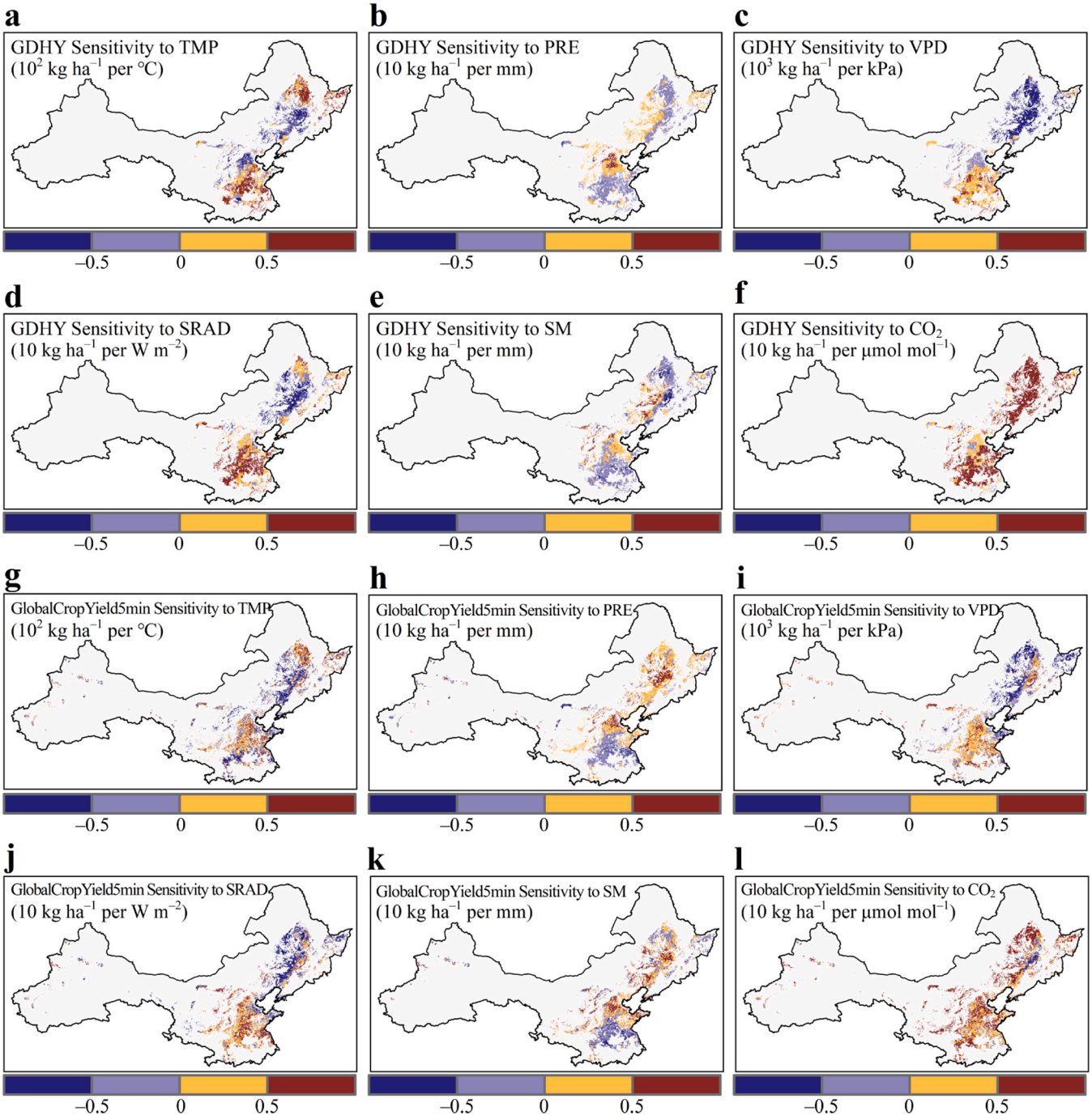

Fig. 6. Spatiotemporal patterns of yield sensitivities to TMP, PRE, VPD, SRAD, SM, and CO_2 for spring and summer maize planting areas in China. (a–f) Spatial distribution of the spring and summer maize's yield sensitivities to TMP, PRE, VPD, SRAD, SM, and CO_2 derived from GDHY during 2000–2016. (g–l) Spatial distribution of the spring and summer maize's SIF sensitivities to TMP, PRE, VPD, SRAD, SM, and CO_2 derived from GlobalCropYield5min during 2000–2015.

to brightening in these regions may result in certain areas or time periods not exhibiting a significant linear trend in SRAD (Shi et al., 2021). In addition, our findings indicated that CO_2 growth rates were greater in the summer planting region compared to the spring planting region. This can be attributed to economic factors such as higher population density, more concentrated urbanization, and increased coal energy consumption (Zheng et al., 2020).

For the spatiotemporal patterns of maize growth under the recent climate and CO_2 trends, this study found that NDVI, SIF, GPP, and yield were increasing across most planting areas in China. However, the significant trends in NDVI, SIF, and GPP were greater for spring maize compared to summer maize. These increases in NDVI, SIF, and GPP within China's maize planting areas were greater than those of global vegetation growth (Song et al., 2022; Zhu et al., 2016). Moreover, the GDHY and GlobalCropYield5min results confirmed that the rates of increase in spring maize yield were mostly higher than summer maize. The advances in agronomic management practices, including more irrigation facilities, higher planting densities, and crop variety updates, have improved China's maize production (Liao et al., 2024; Zhao et al., 2015). In this study, by assigning unquantifiable agronomic management practices-related independent variables to the residual error term, we have ensured the accuracy of sensitivity estimates while accepting the

trade-off of reduced model interpretability (Liu et al., 2019; Song et al., 2022; Yuan et al., 2019). The warming trend in the spring maize planting region during 2000–2020 was relatively weak, resulting in a low risk from high temperatures (Zhao et al., 2016). The increased rainfall during the period also contributed to cooling while satisfying crop water requirements. Heat stress, atmospheric drying, and extreme drought suppressed the increases in NDVI, SIF, and GPP during summer maize growth (Wan et al., 2022; Zhang et al., 2024). Despite the CO_2 fertilization effect being potentially stronger in the summer planting region, maize growth here was constrained by other climate drivers (McGrath and Lobell, 2013; Rezaei et al., 2023). Overall, recent climate change is leading to a continuous gap between spring and summer maize yields (Huang et al., 2021; Tao et al., 2015; Wang et al., 2022).

Our core findings demonstrated that maize growth's sensitivities to climate and CO_2 were statistically significantly different between the spring and summer planting regions in China during 2000–2020. Given that the spring maize planting region was mainly rain-fed, the lack of irrigation could make its crop growth more dependent on PRE (Wan et al., 2022; Zhou et al., 2020a). The increased PRE led to higher SM and concurrently to lower TMP, VPD, and SRAD across the spring planting region. Maize growth here seems to be benefiting from recent climate conditions (Guo et al., 2017; Lu et al., 2025). The increased yields could significantly enhance the sensitivities to climate change, along with greater associated risks (Li et al., 2022). In contrast, the summer maize planting region experienced more challenging climate conditions. The areas have been suffering from significant warming over the past few decades. Although the increases in VPD and SRAD were not statistically significant, heat stress was believed to be one of the key factors limiting further increases in maize growth (Shirazi et al., 2022; Zhang et al., 2021). Meanwhile, these areas had good irrigation conditions, ensuring an adequate water supply in years without extreme drought events. This led to a steady increase in China's summer maize yield, though at a slower pace than spring maize (Wang et al., 2023; Zhang and Lu, 2024). The strategy to ensure stable yields may enable it to become less sensitive to climate change. In addition, both China's spring and summer maize growth showed positive sensitivities to CO_2. The nonlinear CO_2 fertilization effect and changes in water use efficiency may both widen the difference in the sensitivities to CO_2 between the two regions (Song et al., 2024a; Wang et al., 2020; Zhan et al., 2025).

It cannot be denied that the trends based on the active maize growing seasons may not be consistent with those considered for all months throughout the year (Dong et al., 2024; Zhang et al., 2020). We used satellite-observed NDVI, SIF, and GPP as proxies to estimate the trends for China's spring and summer maize growth during the period. The quality of these data and their associated mechanisms with crop growth may be different (Wu et al., 2010). We applied these multiple datasets to enhance the robustness of our findings, yet unavoidable inconsistencies remain in some zones. Meanwhile, we also evaluated the results based on gridded maize yield data, but the lack of standardized ground truth points and the short time series led to poor performance. We found that while both datasets generally indicated increasing trends in maize yields, there was indeed a lack of consistency regarding the exact percentage of significant increases. The discrepancies between the GDHY and GlobalCropYield5min datasets may be attributed to from differences in spatial allocation strategies. GDHY primarily redistributes national statistics using harvested area weights, whereas GlobalCropYield5min incorporates additional spatial heterogeneity constraints. This also led to inconsistencies in their subsequent sensitivity analysis results.

This study deployed machine learning models to estimate the sensitivities of maize growth to climate and CO_2 during the period. This method can reduce the uncertainty caused by changes in the number of independent variables (Song et al., 2024b; Yuan et al., 2019). We tried our best to minimize the effects of not considering crop varieties, planting density, irrigation, and fertilization. However, these human-induced factors may still cause the sensitivities to be over- or under-estimated (Liu et al., 2025a, 2025b; Meng et al., 2016). This suggests that crops exhibit differential responses to climate change under varying cultivation conditions. In addition, the uncertainties associated with the performance of machine learning models may propagate to sensitivity coefficients. A lower model prediction accuracy directly leads to an expanded range of error in sensitivity estimates, thereby reducing their reliability in certain regions. Our RF_{ALL} models generally exhibit R-squared (R^2) values ranging between 0.4 and 0.7 at each grid cell (Fig. S4). We employed the models on a pixel-by-pixel basis, which did not entirely depend on model performance when revealing the spatiotemporal patterns. The synergistic use of NDVI, SIF, GPP, and yield data was applied to examine the consistency of their results in spatial patterns, thereby reducing uncertainties arising from systematic biases caused by data sources. Although these sensitivity estimates may not be highly accurate at a specific pixel, they are of significant importance in uncovering the spatiotemporal patterns for the entire study region.

Since we used the black-box model, our interpretation of the specific effects of each driver on NDVI, SIF, GPP, and yield was much less clear than what structural equation models did (Wang et al., 2019; Zhou et al., 2019). The currently popular explainable machine learning approaches still fall short in providing quantitative sensitivity analysis, offering only information such as importance rankings and positive/negative effects (Hu et al., 2023). Compared to crop growth models, our machine learning-based framework more effectively captures large-scale spatio-temporal heterogeneity, without requiring detailed local inputs such as soil, cultivar, or field management data. However, AI-based models lack the necessary transparency of mechanisms to clearly elucidate the genetic traits and physiological processes, and biophysical pathways. At present, AI-based models are well-suited for assessing the spatio-temporal patterns of crop sensitivities to climate factors, whereas crop growth models better serve to elucidate mechanisms when detailed parameters are available. Therefore, future research should focus on synergistically integrating AI and process-based models, aiming to enhance estimation accuracy while deepening our understanding of the mechanisms behind crop-climate interactions.

Under future climate scenarios, China's spring and summer maize may continue to exhibit differential sensitivities due to their inherent differences in growth duration, temperature adaptability, photosynthetic accumulation, and exposure to risks. It is urgent to address potential adaptive trade-offs between spring and summer maize by adjusting sowing dates, breeding stress-tolerant hybrids, and optimizing management practices. This will provide a foundation for formulating strategies that simultaneously optimize yield potential and stability. When guiding long-term cropping system planning, the northward expansion of summer maize-wheat rotation should be pursued cautiously to prevent yield losses due to climate fluctuations. In addition, contingency plans should be developed to minimize the impacts of extreme events, including droughts and heatwaves.

5. Conclusions

This study used satellite observations and machine learning to reveal differential sensitivities of spring and summer maize growth to recent climate change in China. We found that the growing conditions for spring maize were generally becoming wetter and colder, while those for summer maize were shifting toward drier and warmer. Further analysis confirmed that China's maize growth showed a slower rate of increase in the summer planting region compared to the spring planting region. Eventually, we employed random forest-based simulation experiments to estimate the sensitivities of maize growth to recent climate change. Our findings indicated that spring and summer maize growth had differential sensitivities during the period. Spring maize generally showed higher sensitivities to these drivers compared to summer maize. In summary, our research highlights how China's spring and summer maize growth experience diverse challenges under recent climate

change. For maize production-related sectors, it is crucial to consider climate change impacts according to local conditions when programming food security policies.

CRediT authorship contribution statement

Yang Song: Writing – original draft, Visualization, Validation, Software, Methodology, Investigation, Funding acquisition, Formal analysis, Conceptualization. **Wangyipu Li:** Writing – review & editing, Software, Investigation, Data curation. **Xun Yu:** Writing – review & editing, Software, Resources. **Xianglin Ji:** Writing – review & editing. **Xiaoliang Lu:** Writing – review & editing, Methodology. **Xing Li:** Writing – review & editing. **Chao Zhang:** Writing – review & editing. **Yong He:** Writing – review & editing. **Xiangyuan Wan:** Writing – review & editing, Supervision, Resources, Project administration. **Jing Wang:** Writing – review & editing, Funding acquisition, Conceptualization.

Declaration of Competing Interest

The authors declare the following financial interests/personal relationships which may be considered as potential competing interests: Given his role as Editor, Jing Wang had no involvement in the peer-review of this article and has no access to information regarding its peer-review. Full responsibility for the editorial process for this article was delegated to another journal editor. If there are other authors, they declare that they have no known competing financial interests or personal relationships that could have appeared to influence the work reported in this paper.

Acknowledgments

This research was supported by the National Natural Science Foundation of China (Grant No. 32301395 and 42375194).

Appendix A. Supporting information

Supplementary data associated with this article can be found in the online version at doi:10.1016/j.eja.2026.128106.

Data availability

Data will be made available on request.

References

Abatzoglou, J.T., et al., 2018. TerraClimate, a high-resolution global dataset of monthly climate and climatic water balance from 1958 to 2015. Sci. Data 5, 170191. https://doi.org/10.1038/sdata.2017.191.

Alimagham, S., et al., 2025. Integrating crop models and machine learning for projecting climate change impacts on crops in data-limited environments. Agric. Syst. 228, 104367. https://doi.org/10.1016/j.agsy.2025.104367.

Bi, W.J., et al., 2022. A global 0.05° dataset for gross primary production of sunlit and shaded vegetation canopies from 1992 to 2020. Sci. Data 9 (1), 213. https://doi.org/10.1038/s41597-022-01309-2.

Cai, Y.P., et al., 2019. Integrating satellite and climate data to predict wheat yield in Australia using machine learning approaches. Agric. For. Meteor. 274, 144–159. https://doi.org/10.1016/j.agrformet.2019.03.010.

Cao, J., et al., 2025. Mapping global yields of four major crops at 5-minute resolution from 1982 to 2015 using multi-source data and machine learning. Sci. Data 12 (1), 357. https://doi.org/10.1038/s41597-025-04650-4.

Dong, J., et al., 2024. Analysis of spatial-temporal trends and causes of vapor pressure deficit in China from 1961 to 2020. Atmos. Res. 299, 107199. https://doi.org/10.1016/j.atmosres.2023.107199.

Gao, J., et al., 2019. Effects of climate change on the extension of the potential double cropping region and crop water requirements in Northern China. Agric. For. Meteor. 268, 146–155. https://doi.org/10.1016/j.agrformet.2019.01.009.

Geng, G., et al., 2025. Random forest model that incorporates solar-induced chlorophyll fluorescence data can accurately track crop yield variations under drought conditions. Ecol. Inf. 85, 102972. https://doi.org/10.1016/j.ecoinf.2024.102972.

Guo, E.L., et al., 2017. Assessing spatiotemporal variation of drought and its impact on maize yield in Northeast China. J. Hydrol. 553, 231–247. https://doi.org/10.1016/j.jhydrol.2017.07.060.

Hu, T.X., et al., 2023. Crop yield prediction via explainable AI and interpretable machine learning: dangers of black box models for evaluating climate change impacts on crop yield. Agric. For. Meteor. 336, 109458. https://doi.org/10.1016/j.agrformet.2023.109458.

Huang, M., et al., 2021. Assessing maize potential to mitigate the adverse effects of future rising temperature and heat stress in China. Agric. For. Meteor. 311, 108673. https://doi.org/10.1016/j.agrformet.2021.108673.

Iizumi, T., Sakai, T., 2020. The global dataset of historical yields for major crops 1981–2016. Sci. Data 7 (1), 97. https://doi.org/10.1038/s41597-020-0433-7.

Jacobson, A.R., et al., 2023. NOAA Global Monitoring Laboratory. Carbon CT2022. https://doi.org/10.25925/Z1GJ-3254.

Li, E., et al., 2022. The compound effects of drought and high temperature stresses will be the main constraints on maize yield in Northeast China. Sci. Total Environ. 812, 152461. https://doi.org/10.1016/j.scitotenv.2021.152461.

Li, X., Xiao, J.F., 2019. A global, 0.05-degree product of solar-induced chlorophyll fluorescence derived from OCO-2, MODIS, and reanalysis data. Remote Sens 11 (5), 517. https://doi.org/10.3390/rs11050517.

Liao, D.H., et al., 2024. Changing climate threatens irrigation benefits of maize gross primary productivity in China. Earth's. Future 12 (1), e2022EF003474. https://doi.org/10.1029/2022EF003474.

Liu, S., et al., 2025a. Opposite effect on soil organic carbon between grain and non-grain crops: Evidence from Main Grain Land, China. Agric. Ecosyst. Environ. 379, 109364. https://doi.org/10.1016/j.agee.2024.109364.

Liu, S., et al., 2025b. Mapping previously undetected trees reveals overlooked changes in pan-tropical tree cover. Nat. Commun. 16 (1), 5561. https://doi.org/10.1038/s41467-025-60662-z.

Liu, X., et al., 2019. Global urban expansion offsets climate-driven increases in terrestrial net primary productivity. Nat. Commun. 10 (1), 5558. https://doi.org/10.1038/s41467-019-13462-1.

Liu, Z.X., et al., 2025c. Differences in effects of varying compound extreme temperature and precipitation events on summer maize yield in North China. Agric. Water Manag. 307, 109237. https://doi.org/10.1016/j.agwat.2024.109237.

Lobell, D.B., Azzari, G., 2017. Satellite detection of rising maize yield heterogeneity in the US Midwest. Environ. Res. Lett. 12 (1). https://doi.org/10.1088/1748-9326/aa5371.

Lu, C.X., et al., 2025. Temporal evolution of maize yield spatial heterogeneity in northeast China: shift of dominant factors from human management to climate change. J. Clean. Prod. 519, 145957. https://doi.org/10.1016/j.jclepro.2025.145957.

McGrath, J.M., Lobell, D.B., 2013. Regional disparities in the CO2 fertilization effect and implications for crop yields. Environ. Res. Lett. 8 (1), 014054. https://doi.org/10.1088/1748-9326/8/1/014054.

Meng, Q., et al., 2016. Growing sensitivity of maize to water scarcity under climate change. Sci. Rep. 6 (1), 19605. https://doi.org/10.1038/srep19605.

Niu, Q., et al., 2022. A 30 m annual maize phenology dataset from 1985 to 2020 in China. Earth Syst. Sci. Data 14 (6), 2851–2864. https://doi.org/10.5194/essd-14-2851-2022.

Rezaei, E.E., et al., 2023. Climate change impacts on crop yields. Nat. Rev. Earth & Environ. 4 (12), 831–846. https://doi.org/10.1038/s43017-023-00491-0.

Shi, H., et al., 2021. Surface brightening in eastern and central China since the implementation of the Clean Air Action in 2013: causes and implications. Geophys. Res. Lett. 48 (3), e2020GL091105. https://doi.org/10.1029/2020GL091105.

Shirazi, S.Z., et al., 2022. Estimating potential yield and change in water budget for wheat and maize across Huang-Huai-Hai Plain in the future. Agric. Water Manag. 260, 107282. https://doi.org/10.1016/j.agwat.2021.107282.

Song, L., et al., 2018. Satellite sun-induced chlorophyll fluorescence detects early response of winter wheat to heat stress in the Indian Indo-Gangetic Plains. Glob. Change Biol. 24 (9), 4023–4037. https://doi.org/10.1111/gcb.14302.

Song, Y., et al., 2022. Increased global vegetation productivity despite rising atmospheric dryness over the last two decades. Earth's. Future 10 (7), e2021EF002634. https://doi.org/10.1029/2021EF002634.

Song, Y., et al., 2024a. Elevated CO2 concentrations contribute to a closer relationship between vegetation growth and water availability in the Northern Hemisphere mid-latitudes. Environ. Res. Lett. 19 (8), 084013. https://doi.org/10.1088/1748-9326/ad5f43.

Song, Y., et al., 2024b. Recent water constraints mediate the dominance of climate and atmospheric CO2 on vegetation growth across China. Earth's. Future 12 (6), e2023EF004395. https://doi.org/10.1029/2023EF004395.

Tao, F., et al., 2015. Temporal and spatial changes of maize yield potentials and yield gaps in the past three decades in China. Agric. Ecosyst. Environ. 208, 12–20. https://doi.org/10.1016/j.agee.2015.04.020.

Wan, W., et al., 2022. Spatiotemporal patterns of maize drought stress and their effects on biomass in the Northeast and North China Plain from 2000 to 2019. Agric. For. Meteor. 315, 108821. https://doi.org/10.1016/j.agrformet.2022.108821.

Wang, H.Z., et al., 2023. A sustainable approach to narrowing the summer maize yield gap experienced by smallholders in the North China Plain. Agric. Syst. 204, 103541. https://doi.org/10.1016/j.agsy.2022.103541.

Wang, S., et al., 2020. Recent global decline of CO2 fertilization effects on vegetation photosynthesis. Science 370 (6522), 1295–1300. https://doi.org/10.1126/science.abb7772.

Wang, T., et al., 2022. Impact of climate variability on grain yields of spring and summer maize. Comput. Electron. Agric. 199, 107101. https://doi.org/10.1016/j.compag.2022.107101.

Wang, Y., et al., 2019. Direct and indirect effects of environmental factors on daily CO2 exchange in a rainfed maize cropland-A SEM analysis with 10 year observations. Field Crops Res 242, 107591. https://doi.org/10.1016/j.fcr.2019.107591.
Wen, K., et al., 2019. Recent surface air temperature change over mainland China based on an urbanization-bias adjusted dataset. J. Clim. 32 (10), 2691–2705. https://doi.org/10.1175/JCLI-D-18-0395.1.
Wu, C., et al., 2010. Gross primary production estimation from MODIS data with vegetation index and photosynthetically active radiation in maize. J. Geophys. Res. Atmos. 115 (D12). https://doi.org/10.1029/2009JD013023.
Yang, X., et al., 2015. Potential benefits of climate change for crop productivity in China. Agric. For. Meteor. 208, 76–84. https://doi.org/10.1016/j.agrformet.2015.04.024.
Yu, W., et al., 2024. HIDYM: a high-resolution gross primary productivity and dynamic harvest index based crop yield mapper. Remote Sens. Environ. 311, 114301. https://doi.org/10.1016/j.rse.2024.114301.
Yuan, W., et al., 2019. Increased atmospheric vapor pressure deficit reduces global vegetation growth. Sci. Adv. 5 (8), eaax1396. https://doi.org/10.1126/sciadv.aax1396.
Zhan, W., et al., 2025. Reduced water loss rather than increased photosynthesis controls CO2-enhanced water-use efficiency. Nat. Ecol. Evol. 9 (9), 1571–1584. https://doi.org/10.1038/s41559-025-02761-0.
Zhang, Q., et al., 2021. Hazard assessment of extreme heat during summer maize growing season in Haihe Plain, China. Int. J. Clim. 41 (10), 4794–4803. https://doi.org/10.1002/joc.7099.
Zhang, Y., et al., 2020. Precipitation Trends Over Mainland China From 1961–2016 After Removal of Measurement Biases. J. Geophys. Res. Atmos. 125 (11), e2019JD031728. https://doi.org/10.1029/2019JD031728.
Zhang, Y., et al., 2024. Reduced actual vapor pressure exerts a significant influence on maize yield through vapor pressure deficit amid climate warming. Int. J. Biometeorol. 68 (10), 2041–2048. https://doi.org/10.1007/s00484-024-02727-0.
Zhang, Z.M., Lu, C.H., 2024. Assessing changes in potential yields and yield gaps of summer maize in the North China Plain. Food Energy Secur 13 (1), e489. https://doi.org/10.1002/fes3.489.
Zhao, J., et al., 2015. Effects of climate change on cultivation patterns of spring maize and its climatic suitability in Northeast China. Agric. Ecosyst. Environ. 202, 178–187. https://doi.org/10.1016/j.agee.2015.01.013.
Zhao, N., et al., 2016. Cooling and wetting effects of agricultural development on near-surface atmosphere over Northeast China. Adv. Meteor. 2016 (1), 6439276. https://doi.org/10.1155/2016/6439276.
Zhao, Y., Lobell, D.B., 2017. Assessing the heterogeneity and persistence of farmers' maize yield performance across the North China Plain. Field Crops Res 205, 55–66. https://doi.org/10.1016/j.fcr.2016.12.023.
Zheng, X., et al., 2020. Drivers of change in China's energy-related CO2 emissions. Proc. Natl. Acad. Sci. 117 (1), 29–36. https://doi.org/10.1073/pnas.1908513117.
Zhou, L., et al., 2019. Evapotranspiration over a rainfed maize field in northeast China: How are relationships between the environment and terrestrial evapotranspiration mediated by leaf area? Agric. Water Manag. 221, 538–546. https://doi.org/10.1016/j.agwat.2019.05.026.
Zhou, Z.Q., et al., 2020b. Is the cold region in Northeast China still getting warmer under climate change impact? Atmos. Res. 237, 104864. https://doi.org/10.1016/j.atmosres.2020.104864.
Zhou, Z.Q., et al., 2020a. Assessing spatiotemporal characteristics of drought and its effects on climate-induced yield of maize in Northeast China. J. Hydrol. 588, 125097. https://doi.org/10.1016/j.jhydrol.2020.125097.
Zhu, Z., et al., 2016. Greening of the Earth and its drivers. Nat. Clim. Change 6 (8), 791–795. https://doi.org/10.1038/nclimate3004.